

# Non-linear density evolution from an improved spherical collapse model

Sunu Engineer,<sup>1★</sup> Nissim Kanekar<sup>2★</sup> and T. Padmanabhan<sup>1★</sup>

<sup>1</sup>*Inter-University Centre for Astronomy and Astrophysics, Post Bag 4, Ganeshkhind, Pune 411 007, India*

<sup>2</sup>*National Centre for Radio Astrophysics, Post Bag 3, Ganeshkhind, Pune 411 007, India*

Accepted 1999 November 30. Received 1999 November 30; in original form 1999 August 10

## ABSTRACT

We investigate the evolution of non-linear density perturbations by taking into account the effects of deviations from spherical symmetry of a system. Starting from the standard spherical top hat model in which these effects are ignored, we introduce a physically motivated closure condition which specifies the dependence of the additional terms on the density contrast,  $\delta$ . The modified equation can be used to model the behaviour of an overdense region over a sufficiently large range of  $\delta$ . The key new idea is a Taylor series expansion in  $(1/\delta)$  to model the non-linear epoch. We show that the modified equations quite generically lead to the formation of stable structures in which the gravitational collapse is halted at around the virial radius. The analysis also allows us to connect up the behaviour of individual overdense regions with the non-linear scaling relations satisfied by the two-point correlation function.

**Key words:** cosmology: theory – dark matter – large-scale structure of Universe.

## 1 INTRODUCTION

Analytic modelling of the non-linear phase of gravitational clustering has been a challenging but interesting problem upon which a considerable amount of attention has been bestowed in recent years. The simplest, yet remarkably successful, model for non-linear evolution is the spherical collapse model (SCM, hereafter), which has been applied in the study of various empirical results in the gravitational instability paradigm. Unfortunately, this approach has serious flaws – both mathematically and conceptually. Mathematically, the SCM has a singular behaviour at finite time and predicts infinite density contrasts for all collapsed objects. Conceptually, it is not advisable to model the real Universe as a sphere, in spite of the standard temptations to which theoreticians often succumb. The two issues are, of course, quite related, since, in any realistic situation, it is the deviations from spherical symmetry that lead to virialized stable structures forming. In conventional approaches, this is achieved by an ad hoc method which involves halting the collapse at the virial radius by hand and mapping the resulting non-linear and linear overdensities to each other. This leads to the well-known rule of thumb that, when the linear overdensity is about 1.68, bound structures with non-linear overdensities of about 178 would have formed. The singular behaviour, however, makes the actual trajectory of a spherical system quite useless after the turnaround phase – a price we pay for the arbitrary procedure used in stabilizing the system. However, the truly surprising feature is that, despite its inherent

arbitrariness, the SCM, when properly interpreted, seems to give useful insights into the behaviour of real systems. The Press–Schechter formalism (Press & Schechter 1974), for the abundance of bound structures, uses the SCM implicitly; more recently, it was shown that the basic physics behind the non-linear scaling relations (NSR) obeyed by the two-point correlation function can be obtained from a judicious application of the SCM (Padmanabhan 1996a, 1997). These successes, as well as the inherent simplicity of the underlying concepts, make the SCM an attractive paradigm for studying non-linear evolution in gravitational clustering and motivate one to ask: can we improve the basic model in some manner so that the behaviour of the system after turnaround is ‘more reasonable’?

It is clear from very general considerations that such an approach has to address fairly non-trivial technical issues. To begin with, *exact* modelling of deviations from spherical symmetry is quite impossible since it essentially requires solving the full BBGKY hierarchy. Secondly, the concept of a radius  $R(t)$  for a shell, evolving only as a result of the gravitational force of the matter inside, becomes ill-defined when deviations from spherical symmetry are introduced. Finally, our real interest is in modelling the statistical features of the density growth; whatever modifications we make to the SCM should eventually tie up with known results for the evolution of, for instance, the two-point correlation function. That is, we have to face the question of how best to obtain the *statistical* properties of the density field from the behaviour of a *single* system.

In this paper, we try to address these problems in a limited but focused manner. We tackle the deviations from spherical symmetry by the retention of a term (which is usually neglected)

★ E-mail: sunu@iucaa.emet.in (SE); nissim@ncra.tifr.res.in (NK); paddy@iucaa.emet.in (TP)

in the equation describing the growth of the density contrast. Working in the fluid limit, we show that this term is physically motivated and present some arguments to derive an acceptable form for the same. The key new idea is to introduce a Taylor series expansion in  $(1/\delta)$  (where  $\delta$  is the density contrast) to model the non-linear evolution. We circumvent the question of defining the ‘radius’ of the non-spherical regions by working directly with density contrasts. Finally, we attempt to make the connection with statistical descriptors of non-linear growth, by using the non-linear scaling relations known from previous work. More precisely, we show that the modified equations predict a behaviour for the relative pair velocity (when interpreted statistically) which agrees with the results of  $N$ -body simulations.

This paper is divided into the following sections. The relevant equations describing the SCM are set out in Section 2; we also summarize the physical and ad hoc aspects of the SCM here. Next, we recast the equations into a different form and introduce two functions: (i) a ‘virialization term’ and (ii) a function  $h_{\text{SC}}(\delta)$ , the asymptotic forms of which are easy to determine. The behaviour of  $h_{\text{SC}}(\delta)$  in the presence and absence of the ‘virialization term’ is also detailed here. In Section 4, we present the arguments that give the functional forms for the above term over a large range of  $\delta$ ; we then go on to present the results in terms of a single collapsing body and show how this term stabilizes a collapse which would have otherwise ended up in a singularity in terms of the growth of the density contrast with time. When this term is carried through into the equation for  $R(t)$  for a single system, it can be seen that the radius reaches a maximum and gracefully decreases to a constant, remaining so thereafter. In the standard SCM, the radius decreases from the maximum all the way down to zero, thereby causing the density to diverge. Section 5 summarizes the results and discusses their implications.

## 2 THE SPHERICAL COLLAPSE MODEL

The scales of interest in the current work are much smaller than the Hubble length and the velocities in question are non-relativistic; Newtonian gravity can hence be used for the following analysis. We will consider the case of a dust-dominated,  $\Omega = 1$  universe and treat the system in the fluid limit as being made up of a pressureless dust of dark matter, with a smoothed density,  $\rho_{\text{m}}(t, \mathbf{x})$ , and a mean velocity,  $\mathbf{v}(t, \mathbf{x})$ . (This approach, of course, ignores effects arising from shell crossing and multistreaming; these will be commented on later.)

The density contrast,  $\delta(\mathbf{x}, t)$ , is defined by

$$\rho_{\text{m}}(t, \mathbf{x}) = \rho_{\text{b}}(t)[1 + \delta(\mathbf{x}, t)], \quad (1)$$

where  $\rho_{\text{b}}$  denotes the smooth background density of matter. We define a velocity field  $u^i = v^j/(a\dot{a})$ , where  $v^j$  is the peculiar velocity (obtained after subtracting out the Hubble expansion) and  $a(t)$  denotes the scale factor. Taking the divergence of the field  $u^i$  and writing it as

$$\partial_i u_j = \sigma_{ij} + \epsilon_{ijk}\Omega^k + \frac{1}{3}\delta_{ij}\theta, \quad (2)$$

where  $\sigma_{ij}$  is the shear tensor,  $\Omega^k$  is the rotation vector and  $\theta$  is the expansion, we can manipulate the fluid equations (see, e.g., Padmanabhan 1996b) to obtain the following equation for  $\delta$ :

$$\begin{aligned} \frac{d^2\delta}{da^2} + \frac{3}{2a}\frac{d\delta}{da} - \frac{3}{2a^2}\delta(1+\delta) \\ = \frac{4}{3}\frac{1}{(1+\delta)}\left(\frac{d\delta}{da}\right)^2 + (1+\delta)(\sigma^2 - 2\Omega^2). \end{aligned} \quad (3)$$

The same equation can be written in terms of time  $t$  as

$$\ddot{\delta} - \frac{4}{3}\frac{\dot{\delta}^2}{(1+\delta)} + \frac{2\dot{a}}{a}\dot{\delta} = 4\pi G\rho_{\text{b}}\delta(1+\delta) + \dot{a}^2(1+\delta)(\sigma^2 - 2\Omega^2). \quad (4)$$

This equation turns out to be the same as the one for density contrast in the SCM, except for the additional term  $(1+\delta)\times(\sigma^2 - 2\Omega^2)$ , arising from the angular momentum and shear of the system. To see this explicitly, we introduce a function  $R(t)$  by the definition

$$1 + \delta = \frac{9GMt^2}{2R^3} \equiv \lambda \frac{a^3}{R^3}, \quad (5)$$

where  $M$  and  $\lambda$  are constants. Using this relation between  $\delta$  and  $R(t)$ , equation (4) can be converted into the following equation for  $R(t)$ :

$$\ddot{R} = -\frac{GM}{R^2} - \frac{1}{3}\dot{a}^2(\sigma^2 - 2\Omega^2)R, \quad (6)$$

where the first term represents the gravitational attraction owing to the mass inside a sphere of radius  $R$  and the second gives the effect of the shear and angular momentum.

In the case of spherically symmetric evolution, the shear and angular momentum terms can be set to zero; this gives

$$\frac{d^2R}{dt^2} = -\frac{GM}{R^2} \quad (7)$$

which governs the evolution of a spherical shell of radius  $R$ , collapsing under its own gravity;  $M$  can now be identified with the mass contained in the shell; this is the standard SCM.

At this point, it is important to note a somewhat subtle aspect of these equations. The original fluid equations are clearly Eulerian in nature, i.e. the time derivatives give the temporal variation of the quantities at a fixed point in space. However, the time derivatives in equation (4), for the density contrast  $\delta$ , are of a different kind. Here, the observer is moving with the fluid element and hence, in this, Lagrangian case, the variation in density contrast seen by the observer has, along with the intrinsic time variation, a component that arises as a consequence of his being at different locations in space at different instants of time. When the  $\delta$  equation is converted into an equation for the function  $R(t)$ , the Lagrangian picture is retained; in the SCM, we can interpret  $R(t)$  as the radius of a spherical shell, comoving with the observer. The mass  $M$  within each shell remains constant in the absence of shell crossing (which does not occur in the standard SCM for reasonable initial conditions) and the entire formalism is well defined. The physical identification of  $R$  is, however, not so clear in the case where the shear and rotation terms are retained, as these terms break the spherical symmetry of the system. We will nevertheless continue to think of  $R$  as the ‘effective shell radius’ in this situation, *defined by* equation (5) governing its evolution. Of course, there is no such ambiguity in the *mathematical* definition of  $R$  in this formalism.

Before proceeding further, let us briefly summarize the results of the standard SCM. Equation (7) can be integrated to obtain  $R(t)$  in the parametric form

$$R = \frac{R_1}{2\delta_1}(1 - \cos \theta), \quad (8)$$

$$t = \frac{3t_1}{4\delta_1^{3/2}}(\theta - \sin \theta), \quad (9)$$

where  $R_1$ ,  $\delta_1$  and  $t_1$  are the initial radius, initial density contrast and

initial time, respectively, with  $R_i^3 = (9GM_i^2/2)(1 + \delta_i)^{-1} \approx (9GM_i^2/2)$  for  $\delta_i \ll 1$ . Given  $M$ , there are only two independent constants, namely  $t_i$  and  $\delta_i$ . All the physical features of the SCM can be easily derived from the above solution. Each spherical shell expands at a progressively lower rate against the self-gravity of the system, reaches a maximum radius and then collapses under its own gravity, with a steadily increasing density contrast. The maximum radius,  $R_{\max} = R_i/\delta_i$ , achieved by the shell occurs at a density contrast  $\delta = (9\pi^2/16) - 1 \approx 4.6$ , which is in the ‘quasi-linear’ regime. In the case of a perfectly spherical system, there exists no mechanism to halt the infall, which proceeds inexorably towards a singularity, with all the mass of the system collapsing to a single point. Thus, the fate of the shell [as described by equations (8) and (9)] is to collapse to zero radius at  $\theta = 2\pi$  with an infinite density contrast; this is, of course, physically unacceptable.

In real systems, however, the implicit assumptions, that (i) matter is distributed in spherical shells and (ii) the non-radial components of the velocities of the particles are small, will break down long before infinite densities are reached. Instead, we expect the collisionless dark matter to reach virial equilibrium. After virialization,  $|U| = 2K$ , where  $U$  and  $K$  are, respectively, the potential and kinetic energies; the virial radius can be easily computed to be half the maximum radius reached by the system.

The virialization argument is clearly physically well motivated for real systems. However, as mentioned earlier, there exists no mechanism in the standard SCM to bring about this virialization; hence, one has to introduce by hand the assumption that, as the shell collapses and reaches a particular radius, say  $R_{\max}/2$ , the collapse is halted and the shell remains at this radius thereafter. This arbitrary introduction of virialization is clearly one of the major drawbacks of the standard SCM and takes away its predictive power in the later stages of evolution. We shall now see how the retention of the angular momentum term in equation (6) can serve to stabilize the collapse of the system, thereby allowing us to model the evolution towards  $r_{\text{vir}} = R_{\max}/2$  smoothly.

### 3 THE $H_{\text{SC}}(\delta)$ FUNCTION

As detailed in the previous section, the primary defect of the standard SCM is the ad hoc nature of the stabilization of the shell against its collapse under gravity, which arises on account of the assumption of perfect spherical symmetry, implicit in the neglect of the shear and angular momentum terms. We hence return to equation (3), retain the above terms, and recast the equation into a form more suitable for analysis. Using logarithmic variables,  $D_{\text{SC}} \equiv \ln(1 + \delta)$  and  $\alpha \equiv \ln a$ , equation (3) can be written in the form (the subscript ‘SC’ stands for ‘spherical collapse’)

$$\frac{d^2 D_{\text{SC}}}{d\alpha^2} - \frac{1}{3} \left( \frac{dD_{\text{SC}}}{d\alpha} \right)^2 + \frac{1}{2} \frac{dD_{\text{SC}}}{d\alpha} = \frac{3}{2} [\exp(D_{\text{SC}}) - 1] + a^2(\sigma^2 - 2\Omega^2). \quad (10)$$

It is convenient to introduce the quantity,  $S$ , defined by

$$S \equiv a^2(\sigma^2 - 2\Omega^2), \quad (11)$$

which we shall hereafter call the ‘virialization term’. The consequences of the retention of the virialization term are easy to describe qualitatively. We expect the evolution of an initially spherical shell to proceed along the lines of the standard SCM in the initial stages, when any deviations from spherical symmetry, present in the initial conditions, are small. However, once the

maximum radius is reached and the shell recollapses, these small deviations are amplified by a positive-feedback mechanism. To understand this, we note that all particles in a given spherical shell are equivalent owing to the spherical symmetry of the system. This implies that the motion of any particle, in a specific shell, can be considered representative of the motion of the shell as a whole. Hence, the behaviour of the shell radius can be understood by an analysis of the motion of a single particle. The equation of motion of a particle in an expanding universe can be written as

$$\ddot{X}_i + 2\frac{\dot{a}}{a}\dot{X}_i = -\frac{\nabla\phi}{a^2}, \quad (12)$$

where  $a(t)$  is the expansion factor of the locally overdense ‘universe’. The  $\dot{X}_i$  term acts as a damping force when it is positive, i.e. while the background is expanding. However, when the overdense region reaches the point of maximum expansion and turns around, this term becomes negative, acting like a *negative* damping term, thereby amplifying any deviations from spherical symmetry that might have been initially present. Non-radial components of velocities build up, leading to a randomization of velocities which finally results in a virialized structure, with the mean relative velocity between any two particles being balanced by the Hubble flow. It must be kept in mind, however, that the introduction of the virialization term changes the behaviour of the solution in a global sense and it is not strictly correct to say that this term starts to play a role *only after* recollapse, with the evolution proceeding along the lines of the standard SCM until then. It is nevertheless reasonable to expect that, at early times when the term is small, the system will evolve as the standard SCM to reach a maximum radius, but will fall back smoothly to a constant size later on.

The virialization term,  $S$ , is, in general, a function of  $a$  and  $\mathbf{x}$ , especially since the derivatives in equation (4) are total time derivatives, which, for an expanding universe, contain partial derivatives with respect to both  $\mathbf{x}$  and  $t$  separately. Handling this equation exactly will take us back to the full non-linear equations for the fluid and, of course, no progress can be made. Instead, we will make the Ansatz that the virialization term depends on  $t$  and  $\mathbf{x}$  only through  $\delta(t, \mathbf{x})$ :

$$S(a, \mathbf{x}) \equiv S(\delta(a, \mathbf{x})) \equiv S(D_{\text{SC}}). \quad (13)$$

In other words,  $S$  is a function of the density contrast alone. This Ansatz seems well motivated because the density contrast,  $\delta$ , can be used to characterize the SCM at any point in its evolution and one might expect the virialization term to be a function only of the state of the system, at least to the lowest order. Further, the results obtained with this assumption appear to be sensible and may be treated as a test of the Ansatz in its own framework.

To proceed further systematically, we *define* a function  $h_{\text{SC}}$  by the relation

$$\frac{dD_{\text{SC}}}{d\alpha} = 3h_{\text{SC}}. \quad (14)$$

For consistency, we shall assume the Ansatz  $h_{\text{SC}}(a, \mathbf{x}) \equiv h_{\text{SC}}[\delta(a, \mathbf{x})]$ . The definition of  $h_{\text{SC}}$  allows us to write equation (10) as

$$\frac{dh_{\text{SC}}}{d\alpha} = h_{\text{SC}}^2 - \frac{h_{\text{SC}}}{2} + \frac{1}{2} [\exp(D_{\text{SC}}) - 1] + \frac{S(D_{\text{SC}})}{3}. \quad (15)$$

Dividing (15) by (14), we obtain the following equation for the function  $h_{\text{SC}}(D_{\text{SC}})$ :

$$\frac{dh_{\text{SC}}}{dD_{\text{SC}}} = \frac{h_{\text{SC}}}{3} - \frac{1}{6} + \frac{1}{6h_{\text{SC}}} [\exp(D_{\text{SC}}) - 1] + \frac{S(D_{\text{SC}})}{9h_{\text{SC}}}. \quad (16)$$

If we know the form of either  $h_{\text{SC}}(D_{\text{SC}})$  or  $S(D_{\text{SC}})$ , this equation allows us to determine the other. Then, using equation (14), one can determine  $D_{\text{SC}}$ . Thus, our modification of the standard SCM essentially involves providing the form of  $S_{\text{SC}}(D_{\text{SC}})$  or  $h_{\text{SC}}(D_{\text{SC}})$ . We shall now discuss several features of such a model in order to arrive at a suitable form.

The behaviour of  $h_{\text{SC}}(D_{\text{SC}})$  can be qualitatively understood from our knowledge of the behaviour of  $\delta$  with time. In the linear regime ( $\delta \ll 1$ ), we know that  $\delta$  grows linearly with  $a$ ; hence  $h_{\text{SC}}$  increases with  $D_{\text{SC}}$ . At the extreme non-linear end ( $\delta \gg 1$ ), the system ‘virializes’, i.e. the proper radius and the density of the system become constant. On the other hand, the density  $\rho_b$ , of the background, falls like  $t^{-2}$  (or  $a^{-3}$ ) in a flat, dust-dominated universe. The density contrast is defined by  $\delta = (\rho/\rho_b - 1) \sim \rho/\rho_b$  (for  $\delta \gg 1$ ) and hence

$$\delta \propto t^2 \propto a^3 \quad (17)$$

in the non-linear limit. Equation (14) then implies that  $h_{\text{SC}}(\delta)$  tends to unity for  $\delta \gg 1$ . Thus, we expect that  $h_{\text{SC}}(D_{\text{SC}})$  will start with a value far less than unity, grow, reach a maximum a little greater than one and then smoothly fall back to unity. (A more general situation discussed in the literature corresponds to  $h \rightarrow$  constant as  $\delta \rightarrow \infty$ , though the asymptotic value of  $h$  is not necessarily unity. Our discussion can be generalized to this case and we plan to explore this in a future work.)

This behaviour of the  $h_{\text{SC}}$  function can be given another useful interpretation whenever the density contrast has a monotonically decreasing relationship with the scale,  $x$ , with small  $x$  implying large  $\delta$  and vice versa. Then, if we use a local power-law approximation  $\delta \propto x^{-n}$  for  $\delta \gg 1$  with some  $n > 0$ ,  $D_{\text{SC}} \propto \ln(x^{-1})$  and

$$h_{\text{SC}} \propto \frac{dD_{\text{SC}}}{d\alpha} \propto -\frac{d \ln(1/x)}{d \ln a} \propto \frac{\dot{x}a}{\dot{a}x} \propto -\frac{v}{\dot{a}x}, \quad (18)$$

where  $v \equiv \dot{x}a$  denotes the mean relative velocity. Thus,  $h_{\text{SC}}$  is proportional to the ratio of the peculiar velocity to the Hubble velocity. We know that this ratio is small in the linear regime (where the Hubble flow is dominant) and later increases, reaches a maximum and finally falls back to unity with the formation of a stable structure; this is another argument leading to the same qualitative behaviour of the  $h_{\text{SC}}$  function.

Note that, in the standard SCM (for which  $S = 0$ ), equation (16) reduces to

$$3h_{\text{SC}} \frac{dh_{\text{SC}}}{dD_{\text{SC}}} = h_{\text{SC}}^2 - \frac{h_{\text{SC}}}{2} + \frac{\delta}{2}. \quad (19)$$

The presence of the linear term in  $\delta$  on the right-hand side of the above equation causes  $h_{\text{SC}}$  to increase with  $\delta$ , with  $h_{\text{SC}} \propto \delta^{1/2}$  for  $\delta \gg 1$ . If virialization is imposed as an ad hoc condition, then  $h_{\text{SC}}$  should fall back to unity discontinuously, which is clearly unphysical; the form of  $S(\delta)$  must hence be chosen so as to ensure a smooth transition in  $h_{\text{SC}}(\delta)$  from one regime to another.

As an aside, we would like to make some remarks on the nature of the ‘virialization term’,  $S(\delta)$ , in a somewhat wider context. As is well known, gravitational clustering can be described at three different levels of approximation, by different mathematical techniques. The first approach tracks the clustering by following the true particle trajectories; this is what is done, for example, in  $N$ -body simulations. This method does not involve any approximation (other than the validity of the Newtonian description at the scales of interest); it is, however, clearly analytically intractable. At the next level, one may describe the system by a one-particle

distribution function and attempt to solve the collisionless Boltzmann equation for the distribution function  $f(t, \mathbf{x}, \mathbf{v})$ ; the approximation here lies in the neglect of gravitational collisions, which seems quite reasonable as the time-scale for such collisions is very large for standard dark matter particles. Finally, one can treat the system in the fluid limit described by five functions: the density  $\rho(t, \mathbf{x})$ , mean velocity  $\mathbf{v}(t, \mathbf{x})$  and gravitational potential  $\phi(t, \mathbf{x})$ , thus neglecting multistreaming effects. Our analysis was based on this level of approximation. The key difference between the last two levels of description lies in the fact that the distribution function allows for the possibility of different particle velocities at any point in space (i.e. the existence of *velocity dispersions*), while the fluid picture assumes a mean velocity at each point. It is also known that the gradients in velocity dispersion can provide a kinetic pressure which will also provide support against gravitational collapse. While a detailed analysis of these terms is again exceedingly difficult, one can incorporate the lowest-order effects of the gradient in the velocity dispersion by modifying equation (10) to the form

$$\begin{aligned} \frac{d^2 D_{\text{SC}}}{d\alpha^2} - \frac{1}{3} \left( \frac{dD_{\text{SC}}}{d\alpha} \right)^2 + \frac{1}{2} \frac{dD_{\text{SC}}}{d\alpha} \\ = \frac{3}{2} [\exp(D_{\text{SC}}) - 1] + a^2(\sigma^2 - 2\Omega^2) + f(a, x), \end{aligned} \quad (20)$$

where  $f(a, x)$  contains the lowest-order contributions from the dispersion terms. We can then define

$$S(a, x) = a^2(\sigma^2 - 2\Omega^2) + f(a, x) \quad (21)$$

and again invoke the Ansatz  $S(a, x) \equiv S(\delta)$ . Note that  $S(\delta)$  now contains the lowest-order contributions arising from shell crossing, multistreaming, etc., besides the shear and angular momentum terms, i.e. it contains all effects leading to virialization of the system. We demonstrate explicitly in an appendix that velocity dispersion terms arise naturally in the ‘force’ equation (for the function  $h \equiv -v/\dot{a}x$ ), derived from the BBGKY hierarchy, and play the same role as the function  $S(\delta)$  in the fluid picture. This clearly justifies the above procedure and shows that our approach could have a somewhat larger domain of validity than might be expected from an analysis based on the fluid picture.

#### 4 THE VIRIALIZATION TERM

We will now derive an approximate functional form for the virialization function from physically well-motivated arguments. If the virialization term is retained in equation (6), we have

$$\frac{d^2 R}{dt^2} = -\frac{GM}{R^2} - \frac{H^2 R}{3} S, \quad (22)$$

where  $H = \dot{a}/a$ . Let us first consider the late-time behaviour of the system. When virialization occurs, it seems reasonable to assume that  $R \rightarrow$  constant and  $\dot{R} \rightarrow 0$ . This implies that, for large density contrasts,

$$S \approx -\frac{3GM}{R^3 H^2} \quad (\delta \gg 1). \quad (23)$$

Using  $H = \dot{a}/a = (2/3t)$ , and equation (5),

$$S \approx -\frac{27GMt^2}{4R^3} = -\frac{3}{2}(1 + \delta) \approx -\frac{3}{2}\delta \quad (\delta \gg 1). \quad (24)$$

Thus, the ‘virialization’ term tends to a value of  $(-3\delta/2)$  in the

non-linear regime, when stable structures have formed. This asymptotic form for  $S(\delta)$  is, however, insufficient to model its behaviour over the larger range of density contrast (especially the quasi-linear regime) that is of interest to us. Since  $S(\delta)$  tends to the above asymptotic form at late times, the residual part, i.e. the part that remains after the asymptotic value has been subtracted away, can be expanded in a Taylor series in  $(1/\delta)$  without any loss of generality. Retaining the first two terms of expansion, we write the complete virialization term as

$$S(\delta) = -\frac{3}{2}(1 + \delta) - \frac{A}{\delta} + \frac{B}{\delta^2} + \mathcal{O}(\delta^{-3}). \quad (25)$$

Replacing for  $S(\delta)$  in equation (10), we obtain, for  $\delta \gg 1$ ,

$$3h\delta \frac{dh_{\text{SC}}}{d\delta} - h_{\text{SC}}^2 + \frac{h_{\text{SC}}}{2} + \frac{1}{2} = -\frac{A}{\delta} + \frac{B}{\delta^2}. \quad (26)$$

[It can be easily demonstrated that the first-order term in the Taylor series is alone insufficient to model the turnaround behaviour of the  $h$  function. We will hence include the next higher-order term and use the form in equation (25) for the virialization term. The signs are chosen for future convenience, since it will turn out that both  $A$  and  $B$  are greater than zero.] In fact, for sufficiently large  $\delta$ , the evolution depends only on the combination  $q \equiv (B/A^2)$ . This is most easily seen by rewriting equation (3), replacing  $S(\delta)$  with the above form. Taking the limit of large  $\delta$ , i.e.  $\delta \gg 1$ , and rescaling  $\delta$  to  $\delta/A$ , we obtain

$$\frac{d^2\delta}{db^2} + \frac{3}{2b} \frac{d\delta}{db} - \frac{4}{3\delta} \left(\frac{d\delta}{db}\right)^2 = -\frac{1}{a^2} + \frac{B}{A^2} \frac{1}{a^2\delta} \quad (27)$$

$$= -\frac{1}{a^2} + \frac{q}{a^2\delta}. \quad (28)$$

From the form of the equation it is clear that the constants  $A$  and  $B$  occur in the combination  $q = B/A^2$  and hence the non-linear regime is modelled by a one-parameter family for the virialization term.

Equation (22) can be written as

$$\ddot{R} = -\frac{GM}{R^2} - \frac{4R}{27t^2} \left( -\frac{27GMt^2}{4R^3} - \frac{A}{\delta} + \frac{B}{\delta^2} \right). \quad (29)$$

Using  $\delta = 9GMt^2/2R^3$  and  $B = qA^2$  we may express equation (29) completely in terms of  $R$  and  $t$ . We now rescale  $R$  and  $t$  in the form  $R = r_{\text{vir}}y(x)$  and  $t = \beta x$ , where  $r_{\text{vir}}$  is the final virialized radius (i.e.  $R \rightarrow r_{\text{vir}}$  for  $t \rightarrow \infty$ ), where  $\beta^2 = (8/3^5)(A/GM)r_{\text{vir}}^3$ , to obtain the following equation for  $y(x)$ :

$$y'' = \frac{y^4}{x^4} - \frac{27}{4} q \frac{y^7}{x^6}. \quad (30)$$

We can integrate this equation to find a form for  $y_q(x)$  [where  $y_q(x)$  is the function  $y(x)$  for a specific value of  $q$ ] using the physically motivated boundary conditions  $y = 1$  and  $y' = 0$  as  $x \rightarrow \infty$ , which is simply an expression of the fact that the system reaches the virial radius  $r_{\text{vir}}$  and remains here thereafter.

The results of numerical integration of this equation for a range of  $q$  values are shown in Fig. 1. As expected on physical grounds, the function has a maximum and gracefully decreases to unity for large values of  $x$  [the behaviour of  $y(x)$  near  $x = 0$  is irrelevant since the original equation is valid only for  $\delta \gg 1$ , at least]. For a given value of  $q$ , it is possible to find the value  $x_c$  at which the function reaches its maximum, as well as the ratio  $y_{\text{max}} = R_{\text{max}}/r_{\text{vir}}$ . The time,  $t_{\text{max}}$ , at which the system will reach the maximum radius is related to  $x_c$  by the relation  $t_{\text{max}} = \beta x_c = t_0(1 + z_{\text{max}})^{-3/2}$ , where  $t_0 = 2/(3H_0)$  is the present age of the Universe and  $z_{\text{max}}$  is the redshift at which the system turns around. Fig. 2 shows the variation of  $x_c$  and  $y_{\text{max}} \equiv (R_{\text{max}}/r_{\text{vir}})$  for different values of  $q$ . The entire evolution of the system in the modified spherical collapse model (MSCM) can be expressed in terms of

$$R(t) = r_{\text{vir}} y_q(t/\beta), \quad (31)$$

where  $\beta = (t_0/x_c)(1 + z_{\text{max}})^{-3/2}$ .

In the SCM, the conventional value used for  $(r_{\text{vir}}/R_{\text{max}})$  is  $\frac{1}{2}$ ,

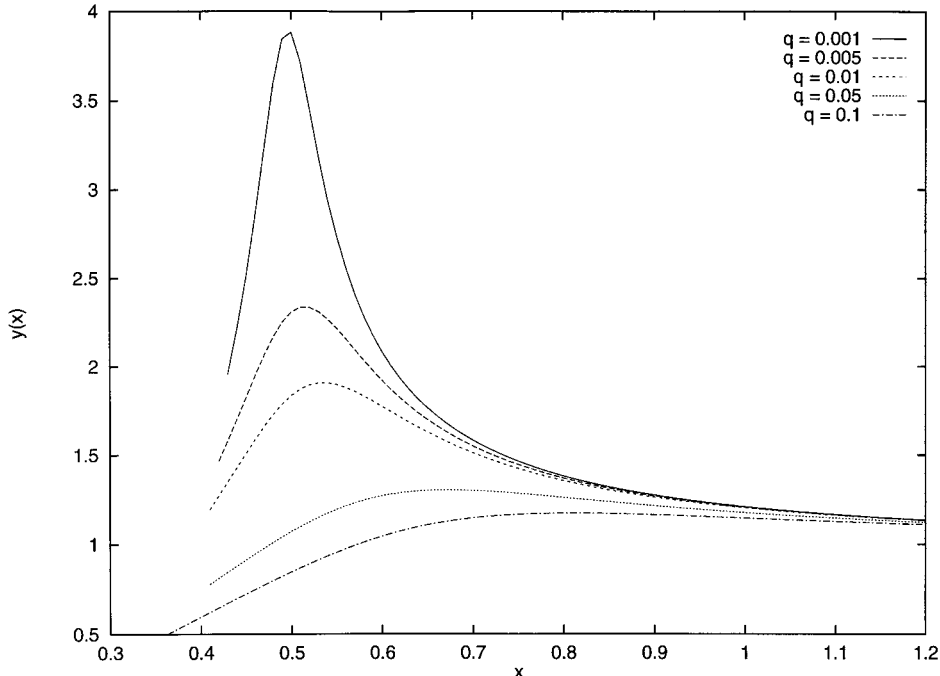
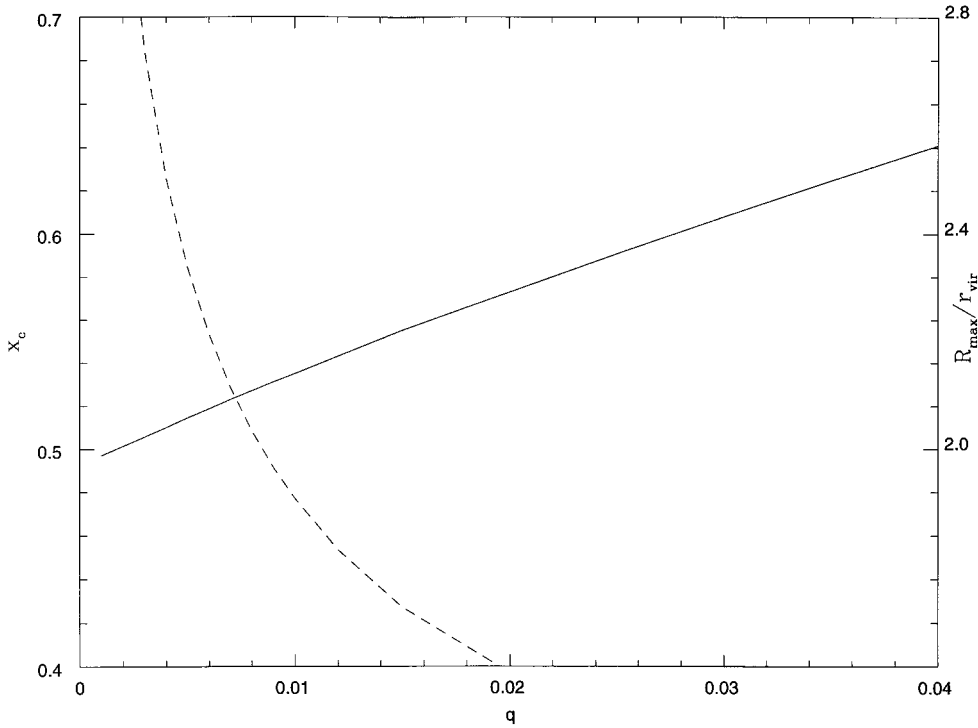


Figure 1. The function  $y_q(x)$  for some values of  $q$ . The  $x$ -axis has scaled time,  $x$ , and the  $y$ -axis is the scaled radius  $y$ .



**Figure 2.** The parameters ( $R_{\max}/r_{\text{vir}}$ ) (broken line) and  $x_c$  (solid line) as a function of  $q = B/A^2$ . This clearly demonstrates that the single-parameter description of the virialization term is constrained by the value that is chosen for the ratio  $r_{\text{vir}}/R_{\max}$ .

which is obtained by enforcing the virial condition that  $|U| = 2K$ , where  $U$  is the gravitational potential energy and  $K$  is the kinetic energy. It must be kept in mind, however, that the ratio ( $r_{\text{vir}}/R_{\max}$ ) is not really constrained to be *precisely*  $\frac{1}{2}$  since the actual value will depend on the final density profile and the precise definitions used for these radii. While we expect it to be around 0.5, some amount of variation, say between 0.25 and 0.75, cannot be ruled out theoretically.

Fig. 2 shows the parameter ( $R_{\max}/r_{\text{vir}}$ ), plotted as a function of  $q = B/A^2$  (dashed line), obtained by numerical integration of equation (22) with the Ansatz (25). The solid line gives the dependence of  $x_c$  (or equivalently  $t_{\max}$ ) on the value of  $q$ . It can be seen that one can obtain a suitable value for the ( $r_{\text{vir}}/R_{\max}$ ) ratio by choosing a suitable value for  $q$  and vice versa. Using equation (14) and the definition  $\delta \propto t^2/R^3$ , we obtain

$$h_{\text{SC}}(x) = 1 - \frac{3}{2} \frac{x}{y} \frac{dy}{dx}, \quad (32)$$

which gives the form of  $h_{\text{SC}}(x)$  for a given value of  $q$ ; this, in turn, determines the function  $y_q(x)$ . Since  $\delta$  can be expressed in terms of  $x$ ,  $y$  and  $x_c$  as  $\delta = (9\pi^2/2x_c^2)x^2/y^3$ , this allows us to obtain a form for  $h_{\text{SC}}(\delta)$  implicitly, determined only by the value of  $q$ .

Fig. 3 shows the behaviour of  $h_{\text{SC}}$  functions obtained by integrating equation (16) backwards, assuming that  $h_{\text{SC}} \rightarrow 1$  as  $\delta \rightarrow \infty$ . It is seen that all the curves have the same turnaround behaviour expected on the basis of the physical arguments presented in the earlier section.

If the functional form for  $h_{\text{SC}}$  – determined, say, from  $N$ -body simulations – is used as a further constraint, we should be able to obtain the values of  $q$ . The major hurdle in attempting to do this is the fact that the available simulation results are given in terms of the averaged two-point correlation function,  $\bar{\xi}$ , and the averaged

pair velocity,  $h(a, x)$ , defined by

$$\bar{\xi} = \frac{3}{r^3} \int_0^r \xi(x, a) x^2 dx, \quad h(a, x) = -\frac{\langle v(a, x) \rangle}{\dot{\alpha}}, \quad (33)$$

where the two-point correlation function  $\xi$  is defined as the Fourier transform of the power spectrum,  $P(k)$ , of the distribution. The results published in the literature assume that  $h(a, x)$  depends on  $a$  and  $x$  only through  $\bar{\xi}(a, x)$ , that is,  $h(a, x) \equiv h[\bar{\xi}(a, x)]$ . This assumption has been invoked previously in several papers (see, e.g., Hamilton et al. 1991; Nityananda & Padmanabhan 1994; Mo, Jain & White 1995; Padmanabhan 1996a; Padmanabhan & Engineer 1998) and seems to be validated by numerical simulations. The fitting formula for  $h(\bar{\xi})$  can be obtained from related fitting formulae available in the literature (e.g. Hamilton et al. 1991). These are, however, statistical quantities and are not well defined for an isolated overdense region. Hence we have first to make the correspondence between  $h_{\text{SC}}(\delta)$  and  $h(\bar{\xi})$ , which we do as follows.

It is possible to show by standard arguments (Nityananda & Padmanabhan 1994) that

$$\frac{d\bar{\xi}}{d\alpha} = 3h(1 + \bar{\xi}); \quad (34)$$

that is,

$$\frac{dD}{d\alpha} = 3h, \quad (35)$$

where  $D = \ln(1 + \bar{\xi})$  and  $\alpha = \ln a$ . Equation (35) is very similar to equation (14), which defines the function  $h_{\text{SC}}(\delta)$ , except for the different definitions of  $D$  and  $D_{\text{SC}}$  in terms of  $\bar{\xi}$  and  $\delta$ , respectively. This suggests that one can obtain a relation between  $h_{\text{SC}}(\delta)$  and  $h(\bar{\xi})$  by relating the density contrast  $\delta$  of an isolated spherical region to the two-point correlation function  $\bar{\xi}$  averaged

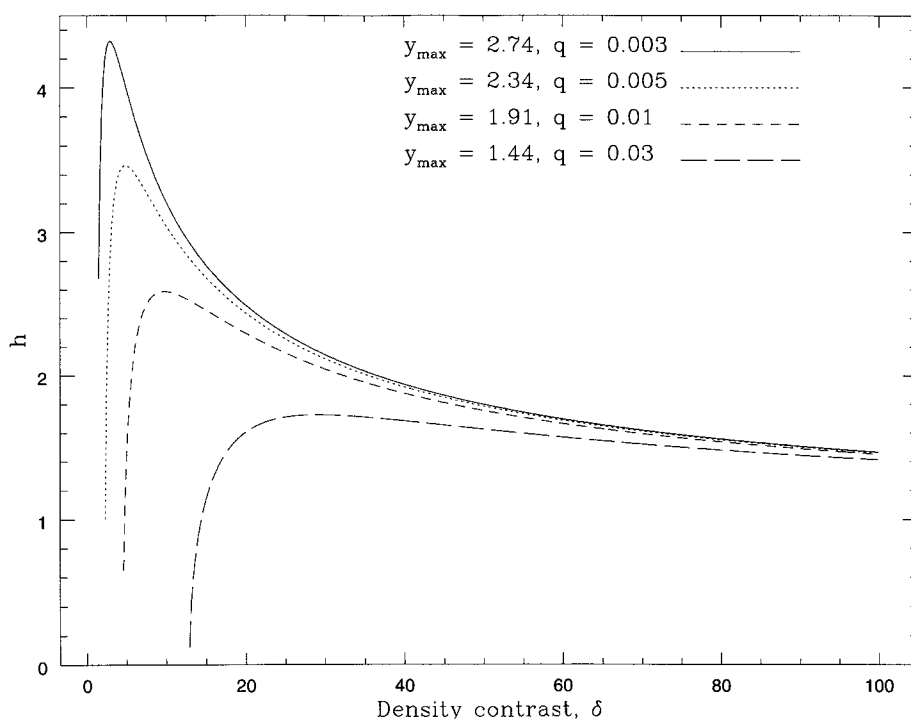


**Figure 3.** The  $h_{\text{SC}}$  function, obtained for various values of  $q$ . The values of  $q$  and  $y_{\text{max}} \equiv R_{\text{max}}/r_{\text{vir}}$  for the curves are indicated at the top right-hand corner. (Further discussion is given in the text.)

over the distribution at the same scale. We essentially need to find a mapping between  $\bar{\xi}$  and  $\delta$  that is valid in a statistical sense.

Gravitational clustering is known to have three regimes in its growing phase, usually called ‘linear’, ‘quasi-linear’ and ‘non-linear’, respectively. The three regimes may be characterized by values of density contrast as  $\delta \ll 1$  in the linear regime,  $1 < \delta < 100$  in the quasi-linear regime and  $100 < \delta$  in the non-linear regime. The three regimes have different rates of growth for various quantities of interest such as  $\delta$ ,  $\xi$  and so on. In the linear regime, it is well known that the density contrast grows proportionally to the scale factor,  $a$ . This implies that the power spectrum,  $P(k) \equiv |\delta_k|^2$  [where  $\delta_k$  is the Fourier mode corresponding to  $\delta(x)$ ], grows as  $a^2$ . Consequently,  $\bar{\xi}$ , which is related to  $P(k)$  via a Fourier transform, also grows as  $a^2$ , i.e. as the square of the density contrast. In the quasi-linear and non-linear regimes, the density contrast does not grow linearly with the scale factor and the relation between  $\delta$  and  $\bar{\xi}$  is not so clearly defined. The quasi-linear regime may be loosely construed as the interval of time during which the high peaks of the initial Gaussian random field have collapsed, although mergers of structures have not yet begun to play an important role. [This idea was used by Padmanabhan (1996a) to model the non-linear scaling relations successfully.] If we consider a length-scale smaller than the size of the collapsed objects, the dominant contribution to  $\bar{\xi}$  (at this scale) arises from the density profiles centred on the collapsed peaks. Using the relation

$$\rho \approx \rho_b(1 + \bar{\xi}) \quad (36)$$

for density profiles around high peaks, one can see that  $\bar{\xi} \propto \delta$  in this regime. In the non-linear regime,  $\delta$  and  $\bar{\xi}$  have the forms  $\delta(a, x) = a^3 F(ax)$ ,  $\bar{\xi} = a^3 G(ax)$ , where  $x$  is a comoving and  $r = ax$  is a proper coordinate. When the system is described by Lagrangian coordinates (which correspond to proper coordinates  $r = ax$ , i.e. at constant  $r$ ),  $\bar{\xi}$  is proportional to  $\delta$ . Thus, the relation

$\bar{\xi} \propto \delta$  appears to be satisfied in all regimes, except at the very linear end. Since we are only interested in the  $\delta > 1$  range, we use  $\bar{\xi} \approx \delta$  and compare equations (34) and (14) to identify

$$h_{\text{SC}}(\delta) \approx h(\bar{\xi}). \quad (37)$$

It is now straightforward to choose the value of  $q$  such that the known fitting function for the  $h$  function is reproduced as closely as possible. We use the original function given by Hamilton et al. (1991) to obtain the following expression for  $h(\bar{\xi})$ :

$$h(\bar{\xi}) = \frac{2}{3} \left[ \frac{d \ln \mathcal{V}(\bar{\xi})}{d \ln(1 + \bar{\xi})} \right]^{-1}, \quad (38)$$

where  $\mathcal{V}(\bar{\xi})$  is given by the fitting function

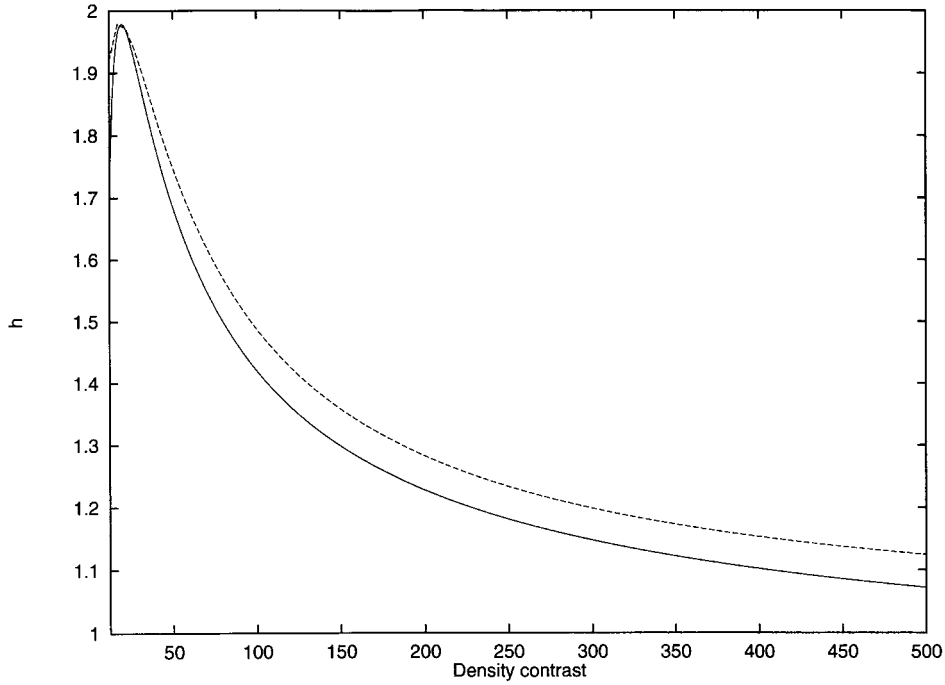
$$\mathcal{V}(\bar{\xi}) = \bar{\xi} \left( \frac{1 + 0.0158 \bar{\xi}^2 + 0.000115 \bar{\xi}^3}{1 + 0.926 \bar{\xi}^2 - 0.0743 \bar{\xi}^3 + 0.0156 \bar{\xi}^4} \right)^{1/3}. \quad (39)$$

Fig. 4 shows the simulation data represented by the fit (solid line) (Hamilton et al. 1991) and the best fit (dashed line), obtained in our model, for  $q \approx 0.02$ . We note that the fit is better than 5 per cent for all values of density contrast  $\delta \geq 15$ . The change in the fit is very marginal if one imposes the boundary condition  $h(\delta) \rightarrow 1$  for  $\delta \gg 1$ , instead of constraining the curves to match at their peaks (for example, the change in the peak height is  $\sim 1$  per cent, if we impose the above condition at  $\delta = 10000$ ).

Fig. 5 shows the plot of scaled radius  $y_q(x)$  versus  $x$ , obtained by integrating equation (30), with  $q = 0.02$ . The figure also shows an accurate fit (dashed line) to this solution of the form

$$y_q(x) = \frac{x + ax^3 + bx^5}{1 + cx^3 + bx^5} \quad (40)$$

with  $a = -3.6$ ,  $b = 53$  and  $c = -12$ . This fit, along with values for  $r_{\text{vir}}$  and  $z_{\text{max}}$ , completely specifies our model through equation (31). It can be observed that  $(r_{\text{vir}}/R_{\text{max}})$  is approximately 0.65. It is



**Figure 4.** The best-fitting curve for the  $h$  function (dashed line) to the simulation data (solid line). The simulation results are obtained from Hamilton et al. (1991) and the fit is obtained by adjusting the value of  $q$  parameter until the curves coincide.

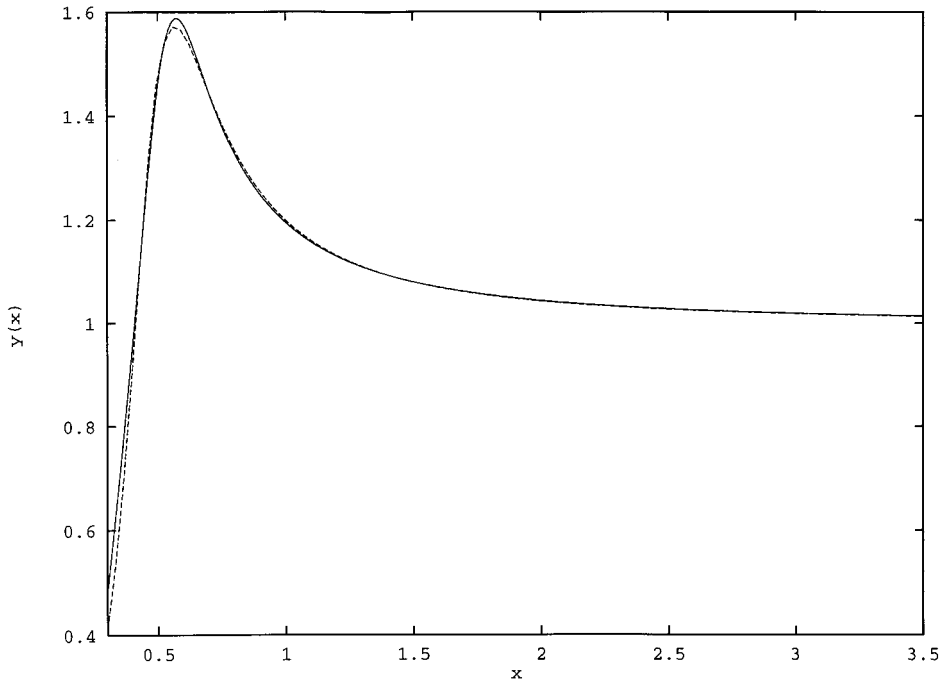


**Figure 5.** A plot of the scaled radius of the shell  $y_q$  as a function of scaled time  $x$  (solid line) and the fitting formula  $y_q = (x + ax^3 + bx^5)/(1 + cx^3 + bx^5)$ , with  $a = -3.6$ ,  $b = 53$  and  $c = -12$  (dashed line) (see the text for a discussion).

interesting to note that the value obtained for the  $(r_{\text{vir}}/R_{\text{max}})$  ratio is not very widely off the usual value of 0.5 used in the standard spherical collapse model, *in spite of the fact that no constraint was imposed on this value, ab initio, in arriving at this result*. Part of this deviation *may* also originate in the fit that has been used for  $h(\xi)$ ; Hamilton et al. (1991) noticed that objects virialized at  $R_{\text{max}}/r_{\text{vir}} \sim 1.8$ , instead of 2, in their simulations.

Finally, Fig. 6 compares the non-linear density contrast in the MSCM (dashed line) with that in the standard SCM (solid line), by plotting both against the linearly extrapolated density contrast,  $\delta_L$ . It can be seen (for a given system with the same  $z_{\text{max}}$  and  $r_{\text{vir}}$ ) that, at the epoch where the standard SCM has a singular behaviour ( $\delta_L \sim 1.686$ ), our model has a smooth behaviour with  $\delta \approx 110$  (the value is not very sensitive to the exact value of  $q$ ).

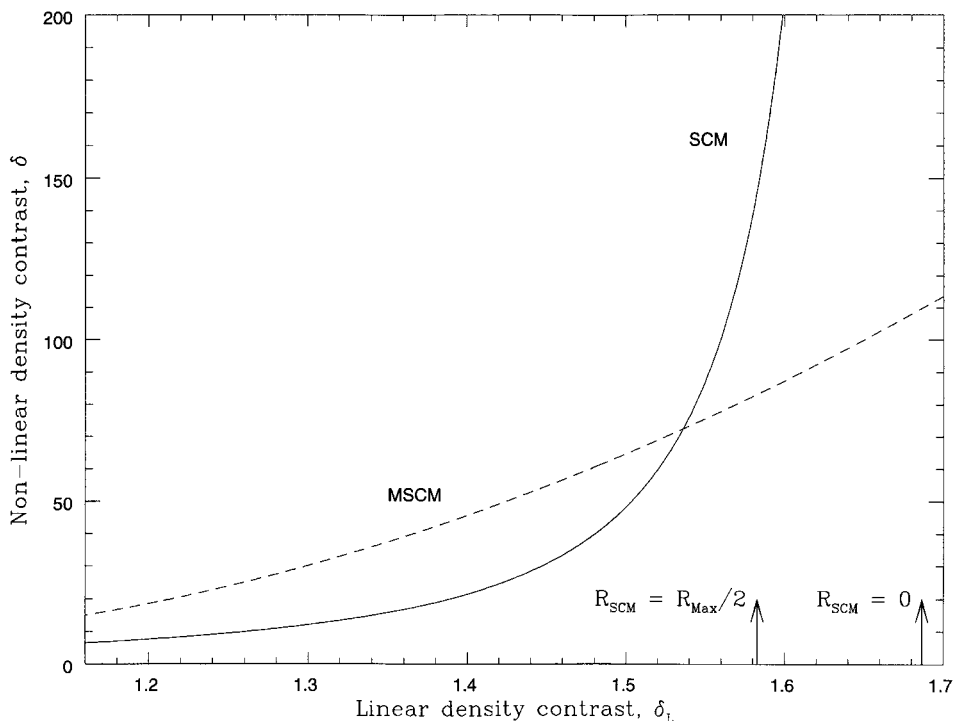


**Figure 6.** The non-linear density contrast in the SCM (solid line) and in the modified SCM (dashed line), plotted against the linearly extrapolated density contrast  $\delta_L$  (a discussion is given in the text).

This is not widely off from the value usually obtained from the ad hoc procedure applied in the standard SCM. In a way, this explains the unreasonable effectiveness of the standard SCM in the study of non-linear clustering.

As mentioned earlier, deviations from spherical symmetry are expected to be small at early epochs and to grow as the system evolves. One would thus expect the two curves of Fig. 6 to approach each other as  $\delta \rightarrow 1$  (from above). Further, the curves should overlies in the linear regime ( $\delta_L \ll 1$ ). It can be seen from the figure that the two curves *do* approach each other as  $\delta_L$  reduces towards unity. However, the MSCM has been obtained using a Taylor expansion in  $(1/\delta)$ ; it is clearly *not* applicable for  $\delta \ll 1$ . Further, the region  $\delta > 15$  has been used to fit the function  $h(\delta)$  to the data of Hamilton et al. (1991). Hence, one cannot compare the curves in the linear regime.

Fig. 6 also shows a comparison between the standard SCM and the MSCM in terms of  $\delta$  values in the MSCM at two important epochs, indicated by vertical arrows. (i) When  $R = R_{\text{max}}/2$  in the SCM, i.e. the epoch at which the SCM *virializes*,  $\delta(\text{MSCM}) \sim 83$ . (ii) When the SCM hits the singularity, ( $\delta_L \sim 1.6865$ ),  $\delta(\text{MSCM}) \sim 110$ .

We note, finally, that Fig. 6, which shows the effects of evolution as a mapping from linear to non-linear density contrasts, contains a subtle implicit assumption regarding the definition of the non-linear density contrast. The radius  $R$  of a system is not a rigorously defined quantity in the absence of spherical symmetry, and obviously any argument involving ‘virialization’ precludes strict spherical symmetry. It is, however, a conventional practice to define the ‘radius’,  $R$ , even for a virialized system without strict spherical symmetry. For example, this approach is used to define the density contrast at ‘virialization’ (which has the value,  $\delta_{\text{vir}} \approx 200$ ) in the standard SCM. In our model we have an explicit equation for  $R$ ; once  $R$  and  $M$  are given, the non-linear density contrast is a well-defined quantity.

## 5 RESULTS AND CONCLUSIONS

In this paper, we have shown how the Taylor expansion of a term in the equation for the evolution of the density contrast,  $\delta$ , in inverse powers of  $\delta$ , allows us to have a more realistic picture of spherical collapse, which is free from arbitrary abrupt ‘virialization’ arguments. Beginning from a well-motivated Ansatz for the dependence of the ‘virialization’ term on the density contrast, we have shown that a spherical collapse model will gracefully turn around and collapse to a constant radius with  $\delta \sim 110$  at the same epoch when the standard model reaches a singularity. Fig. 5 shows clearly that the singularity is avoided in our model owing to the enhancement of deviations from spherical symmetry, and consequent generation of strong non-radial motions.

We derive an approximate functional form for the virialization term starting from the physically reasonable assumption that the system reaches a constant radius. This assumption allows us to derive an asymptotic form for the virialization term, with the residual part adequately expressed by keeping only the first- and second-order terms in a Taylor series in  $(1/\delta)$ . It is shown that there exists a scaling relation between the coefficients of the first- and second-order terms, essentially reducing the virialization term to a one-parameter family of models.

The form of the  $h$  function published in the literature, along with a tentative mapping from  $\delta$  to  $\xi$ , in the non-linear and quasi-linear regimes, allow us to constrain our model further, bringing it in concordance with the available simulation results. Further, it is shown that this form for the virialization term is sufficient to model the turnaround behaviour of the spherical shell and leads to a reasonable numerical value for density contrast at collapse.

There are several new avenues suggested by this work which we plan to pursue in the future.

- (i) The assumption  $h_{\text{SC}} \rightarrow 1$ ,  $R \rightarrow r_{\text{vir}}$  is equivalent to ‘stable

clustering', in terms of the statistical behaviour. Since stable clustering has so far not been proved conclusively in simulations and is often questioned, it would be interesting to see the effect of changing this constraint to  $h \rightarrow \text{constant}$  for  $t \rightarrow \infty$ .

(ii) The technique of Taylor series expansion in  $(1/\delta)$  seems to hold promise. It would be interesting to try such an attempt with the original fluid equations and (possibly) with more general descriptions.

(iii) It must be stressed that we used the  $\delta-\bar{\xi}$  mapping – possibly the weakest part of our analysis, conceptually – only to fix a value of  $q$ . We could have used some high-resolution simulations actually to study the evolution of a realistic overdense region. We conjecture that such an analysis will give results in conformity with those obtained here. We plan to investigate this – thus eliminating our reliance on the  $\delta-\bar{\xi}$  mapping – in a future work.

(iv) Finally, the curves of Fig. 6 can be used to describe the spatial distribution of virialized haloes (see, for example, Mo & White 1996; Sheth 1998). It would be interesting to investigate how things change when the MSCM is used in place of the standard SCM.

## ACKNOWLEDGMENTS

It is a pleasure to thank Ravi Sheth for detailed comments on an earlier version of this paper. SE would like to acknowledge CSIR for support during the course of this work. The research work of one of the authors (TP) was partly supported by the Indo–French Centre for Promotion of Advanced Research under grant contract No 1710-1.

## REFERENCES

- Davis M., Peebles P. J. E., 1977, ApJS, 34, 425  
 Hamilton A. J. S., Kumar P., Lu E., Mathews A., 1991, ApJ, 374, L1  
 Kanekar N., 2000, ApJ, in press (astro-ph/9812203)  
 Mo H. J., White S. D. M., 1996, MNRAS, 282, 347  
 Mo H. J., Jain B., White S. M., 1995, MNRAS, 276, L25  
 Nityananda R., Padmanabhan T., 1994, MNRAS, 271, 976  
 Padmanabhan T., 1996a, MNRAS, 278, L29  
 Padmanabhan T., 1996b, *Cosmology and Astrophysics through Problems*. Cambridge Univ. Press, Cambridge  
 Padmanabhan T., 1997, in Dhurandhar S. V., Padmanabhan T., eds, Proc. ICGC-95 Conf., Gravitation and Cosmology. Kluwer, Dordrecht, p. 37  
 Padmanabhan T., Engineer S. E., 1998, ApJ, 493, 509  
 Press W. H., Schechter P., 1974, ApJ, 187, 425  
 Ruamsuwan L., Fry J. N., 1992, ApJ, 396, 416  
 Sheth R. K., 1998, MNRAS, 300, 1057  
 Yano T., Gouda N., 1997, ApJ, 487, 473

## APPENDIX

The zeroth and first moments of the second BBGKY equation (Ruamsuwan & Fry 1992, equations 22 and 23) can be combined to obtain the following equation for the dimensionless function  $h = -v/\dot{\alpha}x$  (Kanekar 2000):

$$3h(1 + \bar{\xi}) \frac{dh}{d\bar{\xi}} + \frac{h}{2} - h^2 - \frac{3\bar{\xi}}{F} - \frac{9MQe^{-x}}{4\pi F} = h_{\parallel}^2 \left( 4 + \frac{\partial \ln F}{\partial X} \right) + \frac{\partial h_{\parallel}^2}{\partial X} - 2h_{\perp}^2, \quad (\text{A1})$$

where we have used the Ansatz  $h \equiv h(\bar{\xi})$  (Hamilton et al. 1991;

Nityananda & Padmanabhan 1994). In the above, we have defined

$$\bar{\xi}(x, a) = \frac{3}{x^3} \int_0^x dx \xi(x, a)x^2, \quad (\text{A2})$$

$$F = \frac{\partial \bar{\xi}}{\partial X} + 3(1 + \bar{\xi}), \quad X = \ln x, \quad (\text{A3})$$

$$h_{\parallel}^2 = \frac{\Pi}{\dot{a}^2 x^2}, \quad h_{\perp}^2 = \frac{\Sigma}{\dot{a}^2 x^2}, \quad (\text{A4})$$

where  $\Pi$  and  $\Sigma$  are parallel and perpendicular peculiar velocity dispersions (Ruamsuwan & Fry 1992; Kanekar 2000). Finally, we have assumed that the three-point correlation function has the hierarchical form (Davis & Peebles 1977; Ruamsuwan & Fry 1992)

$$\zeta_{123} = Q(\xi_{12}\xi_{13} + \xi_{13}\xi_{23} + \xi_{12}\xi_{23}) \quad (\text{A5})$$

and defined

$$M = \int d^3z [\xi(x) + \xi(z)] \xi(z-x) \frac{\cos \theta}{z^2}. \quad (\text{A6})$$

In the non-linear regime,  $\bar{\xi} \gg 1$ , the stable clustering Ansatz yields a scale-invariant power-law behaviour for  $\bar{\xi}$  (Davis & Peebles 1977), with  $\bar{\xi} \propto a^{(3-\gamma)}x^{-\gamma}$ , if  $h \rightarrow 1$  as  $\bar{\xi} \rightarrow \infty$ . In this limit, we have

$$F = (3 - \gamma)\bar{\xi} + 3 \quad (\text{A7})$$

and

$$\frac{\partial \ln F}{\partial X} = -\gamma \left[ 1 + \left( \frac{3}{3 - \gamma} \right) \left( \frac{1}{\bar{\xi}} \right) \right]^{-1}. \quad (\text{A8})$$

Further, we can write (Yano & Gouda 1997)  $M = M'x\bar{\xi}^2$ , where  $M'$  is a constant. Thus, equation (A1) reduces, in the non-linear regime, to

$$3h\bar{\xi} \frac{dh}{d\bar{\xi}} - h^2 + \frac{h}{2} - \frac{3}{3 - \gamma} \left[ \frac{3M'}{4\pi} \left( \bar{\xi} - \frac{3}{3 - \gamma} \right) + 1 \right] = \left[ (4 - \gamma) + \frac{3\gamma}{(3 - \gamma)\bar{\xi}} \right] h_{\parallel}^2 + \frac{\partial h_{\parallel}^2}{\partial X} - 2h_{\perp}^2 + \mathcal{O}\left(\frac{1}{\bar{\xi}}\right), \quad (\text{A9})$$

where we have retained terms up to order constant in  $\bar{\xi}$ . We now assume that  $h_{\parallel}^2$  and  $h_{\perp}^2$  are functions of  $\bar{\xi}$  alone, to first order. This yields

$$3h\bar{\xi} \frac{dh}{d\bar{\xi}} - h^2 + \frac{h}{2} - \frac{3}{3 - \gamma} \left[ \frac{3M'}{4\pi} \left( \bar{\xi} - \frac{3}{3 - \gamma} \right) + 1 \right] = G(\bar{\xi}) + \mathcal{O}\left(\frac{1}{\bar{\xi}}\right) \quad (\text{A10})$$

with

$$G(\bar{\xi}) = \left[ (4 - \gamma) + \frac{3\gamma}{(3 - \gamma)\bar{\xi}} \right] h_{\parallel}^2(\bar{\xi}) - \gamma\bar{\xi} \frac{dh_{\parallel}^2}{d\bar{\xi}} - 2h_{\perp}^2(\bar{\xi}). \quad (\text{A11})$$

Clearly, if  $h \rightarrow 1$  as  $\bar{\xi} \rightarrow \infty$ , we must have

$$G(\bar{\xi}) = -\frac{3}{3 - \gamma} \left[ \frac{3M'}{4\pi} \left( \bar{\xi} - \frac{3}{3 - \gamma} \right) + 1 \right] - \frac{1}{2} + \mathcal{O}\left(\frac{1}{\bar{\xi}}\right), \quad (\text{A12})$$

i.e.  $G(\bar{\xi}) \approx -9M'\bar{\xi}/4\pi(3 - \gamma)$  for  $\bar{\xi} \gg 1$ .

Since  $G(\bar{\xi})$  tends to the above asymptote at late times, the residual part can be expanded in a Taylor series in  $1/\bar{\xi}$ . Retaining the first two terms of the expansion in equation (A10),

we obtain

$$3h\bar{\xi} \frac{dh}{d\bar{\xi}} - h^2 + \frac{h}{2} + \frac{1}{2} = \frac{A}{\bar{\xi}} + \frac{B}{\bar{\xi}^2} + \mathcal{O}(\bar{\xi}^{-3}). \quad (\text{A13})$$

This is exactly the same as equation (26), with  $\bar{\xi}$  replacing  $\delta$ .  $G(\bar{\xi})$  thus plays the same role as  $S(\delta)$  in the stabilizing of the system against collapse. This clearly implies that the velocity dispersion terms,  $h_{\parallel}^2$  and  $h_{\perp}^2$ , will contribute to the support term; we are hence

justified in writing the virialization term in the more general form

$$S = a^2(\sigma^2 - 2\Omega^2) + f(a, x), \quad (\text{A14})$$

where  $f(a, x)$  contains contributions from effects arising from shell crossing, multistreaming, etc.

This paper has been typeset from a  $\text{\TeX/L\AA\TeX}$  file prepared by the author.